J. Astrophys. Astr. (1986) **7,** 119–129

Extragalactic Sources with Asymmetric Radio Structure II. Further Observations of the Quasar B2 1320 + 299

T. J. Cornwell *National Radio Astronomy Observatory, Post Box 0, Socorro, New Mexico 87801, USA*

D. J. Saikia *Nuffield Radio Astronomy Laboratories, Jodrell Bank, Macclesfield, Cheshire SKI1 9DL, UK** and *Radio Astronomy Centre, Tata Institute of Fundamental Research, Post Box 1234, Bangalore 560012*

P. Shastri *Radio Astronomy Centre, Tata Institute of Fundamental Research, Post Box 1234, Bangalore 560012*

L. Feretti, G. Giovannini, P. Parma *Istituto di Radioastronomia, Via Irnerio 46, I-40126, Bologna, Italy*

C. J. Salter *Institut de Radioastronomie Millimetrique, Avenida Divina Pastora 7, Nucleo Central, 18012 Granada, Spain*

Received 1985 November 21; accepted 1986 March 18

Abstract. We present VLA A-array observations at λ20, 6 and 2 cm and B-array observations at λ20 and 6 cm of the quasar B2 1320 + 299, which has a very unusual radio structure. In addition to a component, A, coincident with the quasar, there are two lobes of radio emission, B and C, on the same side of A. These are located at distances of $\simeq$ 25 and 50 arcsec respectively from A. The present observations show that A has a flat-spectrum component coincident with the quasar and a weak outer component at a distance of $\simeq$4 arcsec along PA $\simeq$ 100°. The morphology of B resembles a head-tail type of structure with its tail towards the north-east. The magnetic field lines in component B appear to follow the bend in the tail. Component C exhibits some extension towards the north-west. We discuss the possible nature of B2 1320 + 299 and suggest that while A appears to be an independent source, the relation between B and C, if they are associated at all, is unclear. Deep optical observations are essential to help clarify the situation.

Key words: extragalactic radio sources—quasars, radio structure—quasars, linear polarization

1. Introduction

The radio source B21320 + 299 (4C 29.48) is associated with a 20th magnitude quasar and has an extremely peculiar radio structure. It consists of two lobes of radio emission, B and C, located on the same side of the component, A, which is coincident with the

* Present address

quasar. B and C are at distances of ≃ 25 and 50 arcsec respectively from A. This source was originally mapped by Fanti *et al.* (1977) and Fanti *et al.* (1979) with the Westerbork Synthesis Radio Telescope (WSRT) at λ6 and 21 cm as part of a programme to make 'short cuts' observations of B2 radio sources identified with quasars. Because of its unusual radio structure, Feretti, Giovannini & Parma (1982) observed this source for 12 hours with the WSRT at λ6 cm, and presented both total-intensity and linear polarization maps at this frequency. They also made linear polarization maps at λ21 cm using the earlier data. Saikia *et al.* observed this source with the VLA C-array at λ6 and 2 cm as part of a project to check the morphological classification of suspected one-sided radio sources, and make a systematic study of their properties. These observations have been described in Paper I of this series (Saikia *et al.* 1984).

Here we present VLA A-array observations at λ20, 6 and 2 cm, VLA B-array observations at λ20 and 6 cm, and discuss the possible nature of this source.

2. Observations and analyses

The A-array observations were made on 25 November 1983 at 1465 (20 cm), 4885 (6 cm) and 14965 (2 cm) MHz, all with a bandwidth of 50 MHz. The source was observed in one scan for ≃ 5 to 10 minutes at each frequency. The B-array observations were made on 12 September 1982 at 1465 and 4885 MHz, for ≃ 30 minutes at each frequency. The bandwidth used was 50 MHz. The primary flux-density and polarization calibrator for all the observations was 3C 286. The flux densities are on the BGPW scale (Baars *et al.* 1977). The data were edited and calibrated via standard computer programmes available at the VLA. All maps presented here have been made from self-calibrated data bases (Schwab 1980), The λ2 cm map has been made from a self-calibrated data base assuming an initial point source model. The observational parameters for the different scans are summarized in Table 1.

3. Results

In Figs 1 and 2 we show the λ20 cm maps of 1320 + 299 made from the B- and A-array data respectively, while in Fig. 3 we present the λ6 cm B-array map. The three components which we label A, B and C appear well separated in all the maps with no bridge or jet connecting any of them. In the A-array observations at the higher frequencies; we detect all the components A, B and C at λ6 cm but only A at λ2 cm. These maps are presented in Figs 4 and 5 respectively. In all figures, the linear polarization is shown by line segments superposed on the total intensity contours. The flux density and polarization properties of the three components are summarized in Table 2 which is self explanatory. The peak flux density of component A at λ2 cm is expected to be ≃ 20 per cent low due to bandwidth smearing. Polarized flux density has been detected in all the three components, in agreement with previous results. It should be noted that the percentage polarization on the maps could depend considerably on the array used even at the same frequency since the components are not point sources and resolution and *uv* coverage vary with the array configuration.

Component A which appears associated with the quasar exhibits a one-sided radio morphology. It consists of a prominent radio core with a weak outer component at a

Table 1. The observational parameters.

Frequency (MHz)	1465	1465	4885	4885	14965
Array configuration	B	A	B	A	A
Bandwidth (MHz)	50	50	50	50	50
Pointing RA (1950)	$13^h\ 20^m\ 40^s.5$	$13^h\ 20^m\ 42^s.17$	$13^h\ 20^m\ 40^s.5$	$13^h\ 20^m\ 42^s.17$	$13^h\ 20^m\ 42^s.17$
Dec (1950)	29° 57′ 23″.0	29° 57′ 12″.0	29° 57′ 23″.0	29° 57′ 12″.0	29° 57′ 12″.0
Synthesized beam					
$\theta_1 \times \theta_2$ ($arcsec^2$)	3.31 × 2.95	1.24 × 1.22	1.20 × 1.15	0.37 × 0.36	0.12 × 0.11
PA (deg)	9	42	129	35	34
rms noise (mJy/beam)	0.30	0.27	0.22	0.25	0.39

Table 2. Flux density and polarization of the individual components.

			λ20 cm		λ6 cm		λ2 cm
		Comp	B-array	A-array	B-array	A-array	A-array
S_{peak}, (mJy/beam)	S_{total} (mJy)	A	379,427	330,385	260,270	210,260	140,160
		B	511,669	330,645	120,229	75,250	
		C	213,247	140,225	49,73	24,80	
Polarization*, (per cent)	PA (deg)	A	2.6,138	5.0,130	4.1,120	5.5,132	5.5,125
		Bw	1.5,167	~ 1,141	12.5,111	18.5,105	
		Be	3.5,61	~ 10 − 15, ~ 70	6.2,20		
		C	9.5,21	9.5,21	9.5,8	9.5,4	

* The quoted A-array values of percentage polarization represent the values at the peak of total intensity. The B-array values of percentage polarization are derived from values of the Stokes parameters Q and U integrated over the relevant component.

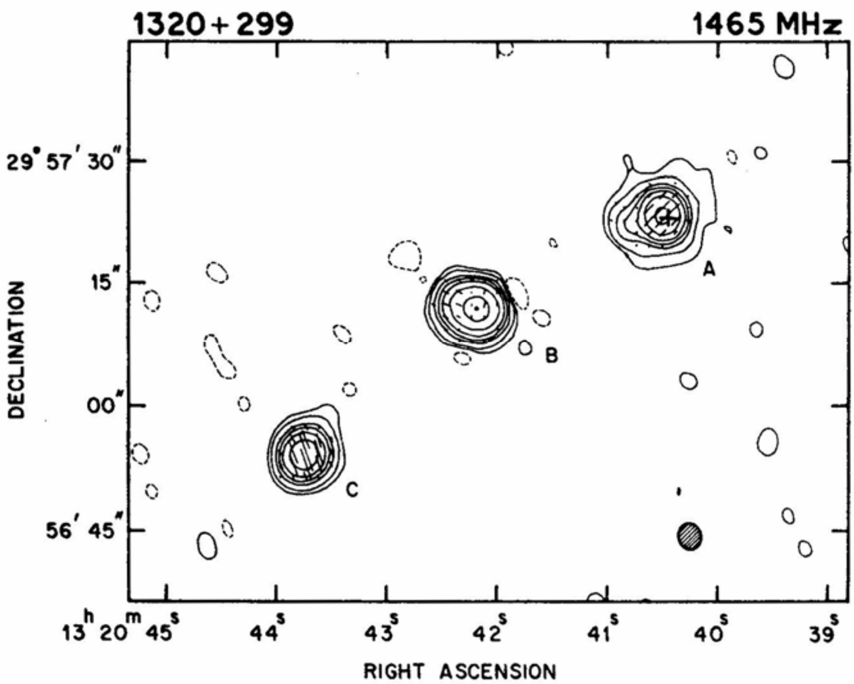

Figure 1. The B-array λ20 cm map of 1320 + 299. Beam: 3.31 × 2.95 $arcsec^2$ along PA 9° .Peak brightness: 511mJy/beam. Contour levels: –1, 1, 3, 10, 20, 40, 100, 300, 500 mJy/beam. Polarization: 1 arcsec = 4.5 mJy/beam. In Figs 1 to 5 the position of the optical quasar is marked by a cross while the beam is shown by a hatched ellipse. The polarization is shown by line segments superposed on the total-intensity contours.

distance ≃ 4 arcsec along PA ≃ 100°. These are connected by a jet-like extension. Using the peak flux densities of the λ6 cm B-array and λ20 cm A-array maps, we find a spectral index for the core of $\alpha_c \simeq 0.2$ ($S \propto \nu^{-\alpha}$). The spectral index between λ6 and 2 cm, using the A-array data is also ≃ 0.2. The integrated λ2 cm flux density has been used to eliminate the effects of bandwidth smearing.

From the A-array data, component A appears to be ≃ 5 per cent polarized at λ20,6 and 2 cm. Clearly there is very little depolarization. The rotation measure estimated from the similar resolution B-array λ6 cm and A-array λ20 cm data is also low, the value being ≃ 5 rad m^{-2}. The *E*-vector at λ6 cm (A-array) is inclined at an angle of 30° to the jet like extension. Using VLA A-array data for a large sample of sources, Saikia & Shastri (1984) have shown that for the one-sided, core-dominated sources, there is no relation between the relative orientation of the core polarization *E*-vector at λ6 cm and the radio axis, while for the classical weak cored double-lobed sources the E-vector tends to be perpendicular to the structural elongation. Assuming that the *E*-vector is tracing the direction of the nuclear jet, the large observed misalignments in the core-dominated sources is perhaps due to amplification of small intrinsic misalignments between the nuclear and larger scale structure by projection effects.

Component B has an extremely interesting asymmetric structure which is well seen in Fig. 4b. There is a high brightness head and a tail which bends towards the north-east and extends up to a distance of ≃ 3 arcsec from the peak. The magnetic field orientation

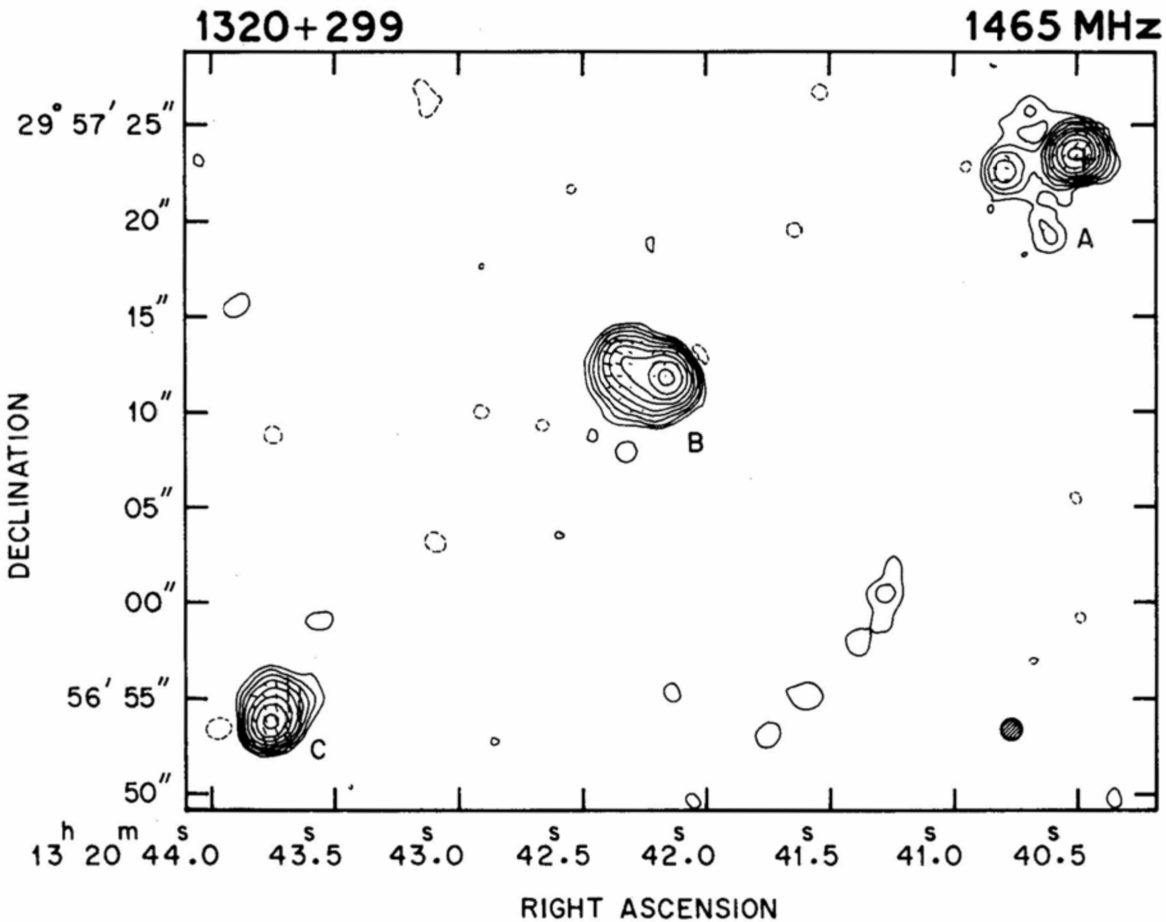

Figure 2. The A-array λ20 cm map of 1320 + 299. **Beam**: 1.24 × 1.22 arcsec^2 along **PA** 42°. **Peak** brightness: 329 mJy/beam. Contour levels: −4, −2, −1, 1, 2, 4, 8, 16, 32, 64, 128, 256 mJy/beam. Polarization: 1 arcsec = 26 per cent.

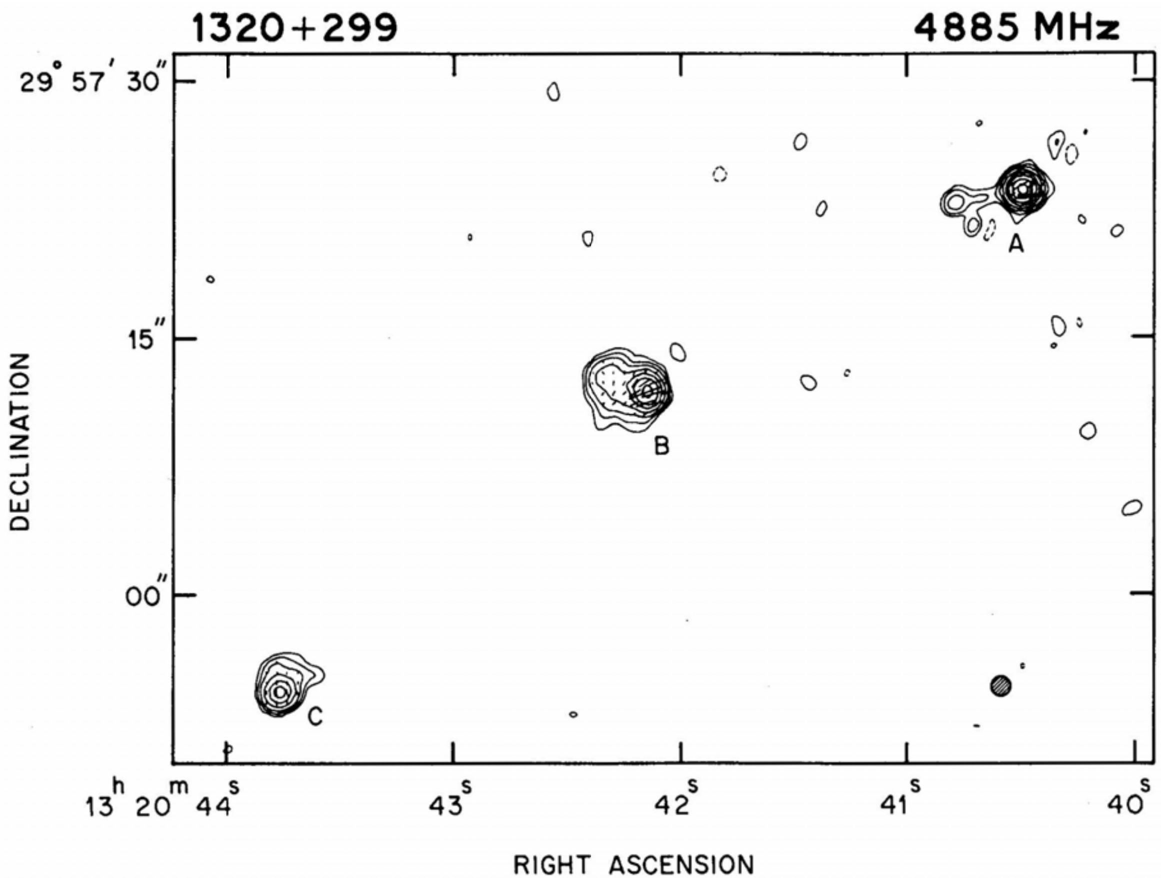

Figure 3. The B-array $\lambda 6$ cm map. Beam: 1.20×1.15 arcsec^2 along PA 129°. Peak brightness: 251 mJy/beam. Contour levels: −0.7, 0.7, 1.4, 3, 8, 20, 40, 100, 200 mJy/beam. Polarization: 1 arcsec = 9.1 mJy/beam.

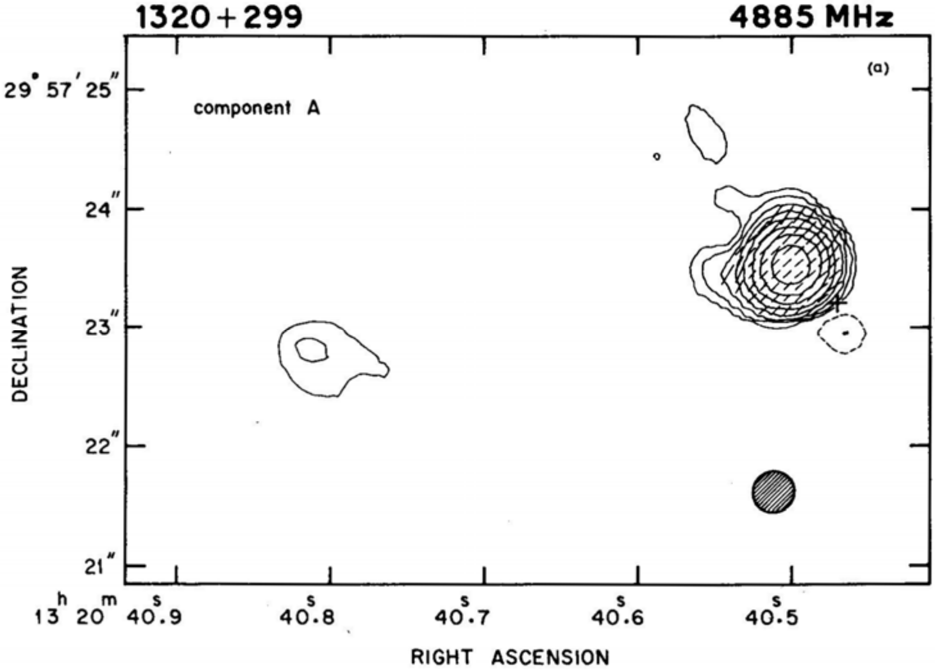

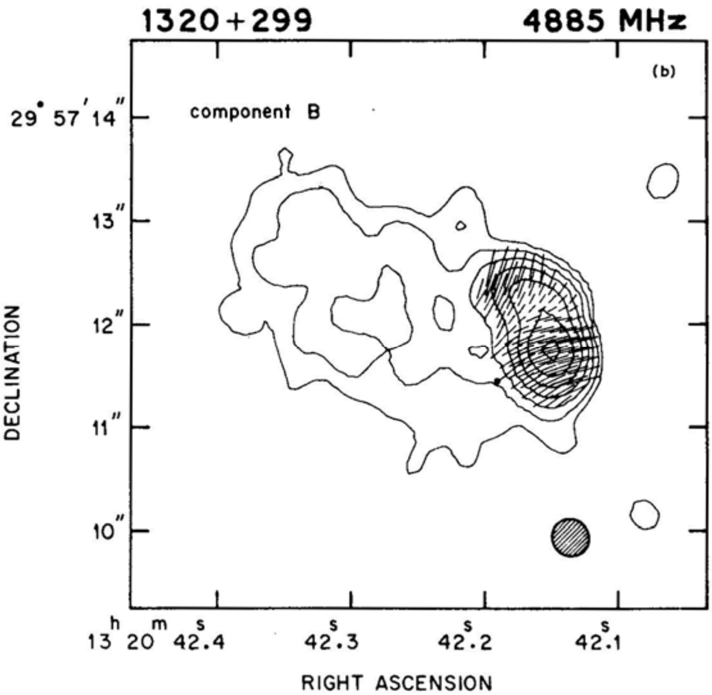

Figure 4. (a) The A-array λ6 cm map of component A. Peak brightness: 210 mJy/beam. Contour levels: –4, –2, –1, 1, 2 ,4, 8, 16, 32, 64, 128 mJy/beam. Polarization: 1 arcsec = 61 per cent. Beam: 0.37 × 0.36 $arcsec^2$ along PA 35° in Figs 4a, b and c. (b) The λ6 cm A-array map component B. Peak brightness: 75 mJy/beam. Contour levels, –4 , –2 , –1, 1, 2, 4, 8, 16, 32, 64 mJy/beam. Polarization: 1 arcsec = 61 per cent.

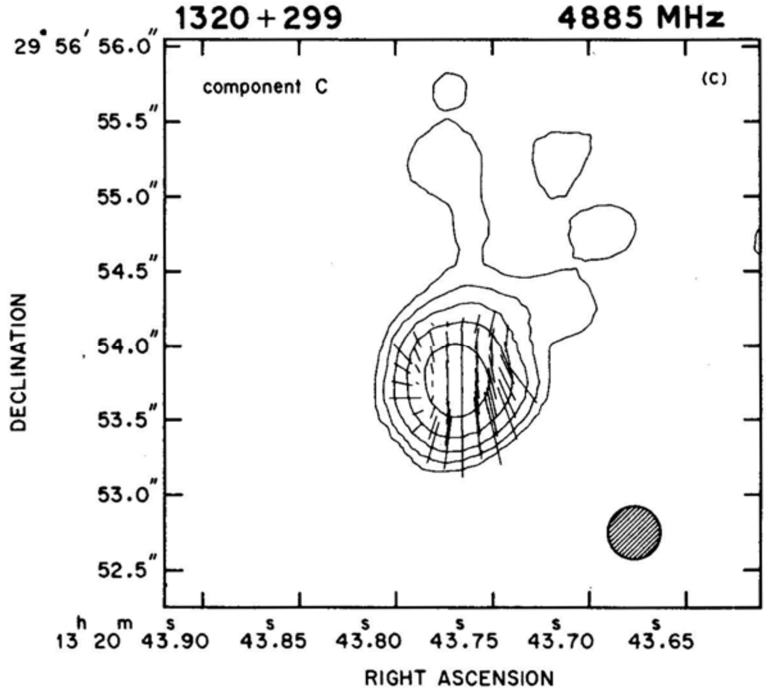

Figure 4. (c) The $\lambda 6$ cm A-array map of component C. Peak brightness: 24 mJy/beam. Contour levels: –4, –2, – 1, 1, 2, 4, 8, 16 mJy/beam. Polarization: 1 arcsec = 61 per cent.

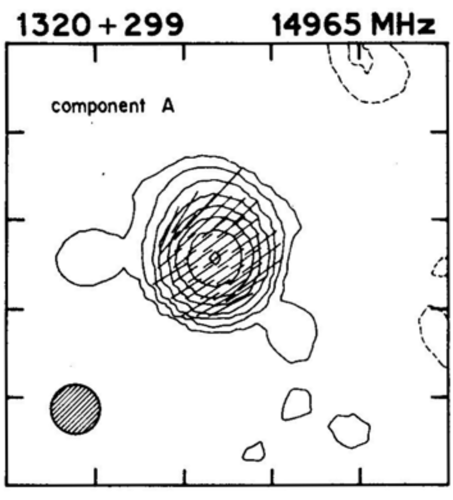

Figure 5, The $\lambda 2$ cm A-array map of component A. Beam: 0.12 × 0.11 arcsec^2 along PA 34°. Peak brightness: 140 mJy/beam. Contour levels: –4, –2, –1, 1, 2, 4, 8, 16, 32, 64, 128 mJy/beam. Polarization: 1 arcsec = 80 per cent. The tick marks are 0.2 arcsec apart.

inferred from the $\lambda 6$ cm data appears to follow the bend, changing by $\simeq 90°$ from west to east. The polarization parameters for the western (Bw) and eastern (Be) parts of B, *i.e* the head and tail respectively, are listed separately in Table 2. The degree of polarization at the pixel of maximum brightness at $\lambda 6$ cm (A-array) is $\simeq 19$ per cent along PA $\simeq 105°$. This value is quite high for a core: the median values of percentage polarization at $\simeq \lambda 6$ cm for cores in galaxies and quasars observed with the VLA A-array are $\simeq 0.5$ and 2 respectively (Saikia, Swarup & Kodali 1985). If the source is really a head-tail type of source, the high brightness strongly polarized feature could indicate that the core has not been adequately resolved in the $\lambda 6$ cm map, and the structure of the head is more complicated.

The rotation measure for the western and eastern parts of B using again the similar resolution B-array $\lambda 6$ cm and A-array $\lambda 20$ cm data is $\simeq 15$ and 25 rad m^{-2} respectively. The peak in the brightness distribution of B appears strongly polarized at $\lambda 6$ cm, but depolarizes considerably at $\lambda 20$ cm. The high degree of polarization seen at $\lambda 6$ cm is consistent with the $\lambda 2$ cm C-array observations of Saikia *et al.* (1984), who report a polarization of 16.9 per cent.

Component C shows a slightly extended feature along the NW direction, which is clearly visible in the maps made with a resolution of $\simeq 1.2$ arcsec (A-array $\lambda 20$ cm and B array $\lambda 6$ cm). The extended feature is also seen in the A-array $\lambda 6$ cm map. The degree of polarization at the pixel of maximum brightness is $\simeq 10$ per cent at both $\lambda 6$ and 20 cm indicating no significant depolarization. The rotation measure is $\simeq$ 5 rad m^{-2} using the λ 20 cm A-array and $\lambda 6$ cm B-array data.

The spectra of components A, B and C are shown in Fig. 6. The integrated spectral index of the complete source is 0.64 ± 0.03 between $\simeq$ 80 MHz and 15 GHz, while the spectral indices of A, B and C are 0.42 ± 0.07, 1.12 ± 0.14 and 0.92 ± 0.02 respectively. While evaluating the spectral indices of the components, we have used the lowest resolution VLA maps at $\lambda 20$, 6 and 2 cm. Component A, which is dominated by a compact core has a flat spectrum while B and C have steep spectra.

4. Discussion

The principal question regarding this source relates to an understanding of whether the three components A, B and C are physically related. Although the probability of three unrelated sources so aligned by chance is extremely low, there is no evidence from the radio data alone of any physical association. The probability of an unrelated source. with $\lambda 20$ cm flux density between $\simeq$ 250 and 450 mJy lying within $\simeq$ 25 arcsec of component B is $\simeq 5 \times 10^{-5}$.

The radio morphology of component A, which is associated with the quasar, is quite similar to that of many core-dominated radio sources which have been mapped with high angular resolution at the VLA and MERLIN (Perley, Fomalont & Johnston 1982; Perley 1982; Browne *et al.* 1982). These sources are characterized by flat and complex spectra, variability of flux density and small angular size, with radio emission often being detected on only one side of the nucleus. Using the available data, it is difficult to establish convincingly that the radio core of component A is variable. However, we note that by comparing the images of the quasar in the PSS prints and in a plate taken by Braccesi in December 1967 with the Palomar Schmidt telescope, Feretti *et al.* (1982) have suggested that the quasar is optically variable.

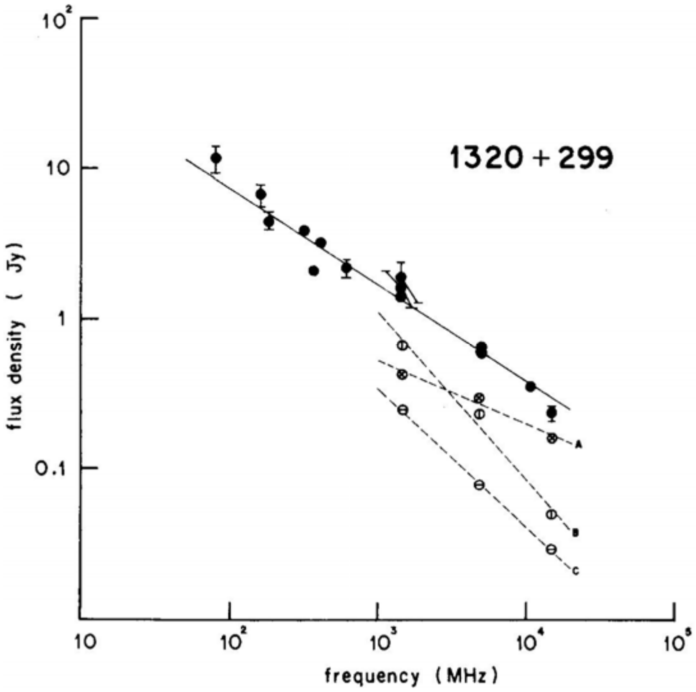

Figure 6. Spectra of the entire source and of the components A, B and C. The flux densities are on the BGPW scale (Baars *et al.* 1977). The different flux densities are represented as follows: ● : entire source,. ⊗ : component A, ⦶ : component B and ⊖: component C. Flux densities for the individual components are taken from the present data or Saikia *et al.* (1984).

Further, assuming that the redshift is $\lesssim$ 2, the total linear extent of A is $\lesssim$30 kpc in an Einstein–de-Sitter universe with H_0 = 50 km s^{-1} Mpc^{-1}. This is similar to the sizes of other sources in this category, and also consistent with the possibility that they are perhaps inclined at small angles to the line of sight (*cf.* Kapahi 1981; Saikia 1985 and references therein).

The radio morphology of component B is reminiscent of a head-tail source, but it could perhaps also be one of the outer components of a double-lobed source. There is no optical object visible on the PSS prints at the position of B, indicating that if B is indeed identified with a galaxy its redshift should be $\gtrsim$ 0.3. Its radio luminosity at 1.4 GHz would then be $\gtrsim$ 2 × 10^{25} W Hz^{-1} sr^{-1} , making it an extremely luminous head-tail source (*cf* O'Dea & Owen 1985). In this picture, an unresolved radio core may not have been detected in the head due to the presence of the high-brightness highly polarized feature in its vicinity.

One has now to understand whether C is an independent source or related to either A or B? Its appearance is somewhat similar to that of an edge-brightened hot-spot, and its small tail is approximately in the north-west direction. Association with A is extremely unlikely since A can be very well classified as an independent source and there is no suggestion of any physical relation. Also, its angular size, and hence the inferred linear size, would be much too large for one-sided radio sources. If B is a separate head-tail source, then A, B and C are independent sources. An exciting explanation of their mutual proximity could be that B and C are identified with faint galaxies belonging to a very distant cluster beyond the limit of the PSS prints containing the quasar A. Another possibility is that B and C are the outer components of a double-lobed radio source whose optical identification is beyond the PSS limit. Deep optical observations should help distinguish between the different possibilities.

Acknowledgements

We thank the staff of the National Radio Astronomy Observatory for help during the observations and S. Krishnamohan for his comments on the manuscript. One of us (DJS) thanks IAU Commission 38 for travel support. The National Radio Astronomy Observatory is operated by Associated Universities Inc. under contract with the National Science Foundation.

References

Baars, J. W. M., Genzel, R., Pauliny-Toth, I. I. K., Witzel, A. 1977, *Astr. Astrophys.,* **61**, 99.

Browne, I. W. A., Orr, M. J. L., Davis, R. J., Foley, A., Muxlow, T. W. B., Thomasson, P. 1982, *Mon. Not. R. astr. Soc,* **198**, 673

Fanti, C, Fanti, R., Formiggini, L., Lari, C., Padrielli, L. 1977, *Astr. Astrophys. Suppl. Ser.,* **28**, 351.

Fanti, R., Feretti, L., Giovannini, G., Padrielli, L. 1979, *Astr. Astrophys. Suppl. Ser.,* **35**, 169.

Feretti, L., Giovannini, G., Parma, P. 1982, *Astr. Astrophys.,* **115**, 423.

Kapahi, V. K. 1981, *J. Astrophys. Astr.,* **2**, 43.

O'Dea, C P., Owen, F. N. 1985, *Astr. J.,* **90**, 954.

Perley, R. A. 1982, *Astr. J.,* **87**, 859.

Perley, R. A., Fomalont, E. B., Johnston, K. J. 1982, *Astrophys. J.,* **255**, L93.

Saikia, D. J. 1985, in *Extragalactic Energetic Sources,* Ed. V. K. Kapahi, Indian Academy of Sciences, Bangalore, p. 105.

Saikia, D. J., Shastri, P. 1984, *Mon. Not. R. astr. Soc,* **211**, 47.

Saikia, D. J. ,Shastri, P., Sinha, R. P., Kapahi, V. K., Swarup, G. 1984, *J. Astrophys. Astr.,* **5**, 429 (Paper I),

Saikia, D. J., Swarup, G., Kodali, P. D. 1985, *Mon. Not. R. astr. Soc,* **216**, 385.

Schwab, F. R. 1980, in *Proc. Int. Optical Computing Conf.,* Ed. W. T. Rhodes: *Proc. Soc. Photo-opt. Instrum. Eng.,* **231**, 18.